Modeling of Low Concentrated Buffer DNA Detection with Suspend Gate Field-Effect Transistors (SGFET)

T. Windbacher, V. Sverdlov, and S. Selberherr
Institute for Microelectronics, TU Wien, Gußhausstraße 27–29, A-1040 Vienna, Austria
e-mail:{Windbacher|Sverdlov|Selberherr}@iue.tuwien.ac.at

***Abstract*—The experimental data of a suspend gate field-effect transistor (SGFET) have been analyzed with three different models. A SGFET is a MOSFET with an elevated gate and an empty space below it. The exposed gate-oxide layer is biofunctionalized with single stranded DNA, which is able to hybridize with a complementary strand. Due to the intrinsic charge of the phosphate groups (minus one elementary charge per group) of the DNA, large shifts in the transfer characteristics are induced. Thus label-free, time-resolved, and in-situ detection of DNA is possible. It can be shown that for buffer concentrations below mmol/l the Poisson-Boltzmann description it is not valid anymore. Because of the low number of counter ions at small buffer concentrations, the screening of the oligo-deoxynucleotides/DNA is more appropriately described with the Debye-Hückel model. Additionally we propose an extended Poisson-Boltzmann model which takes the closest possible ion distance to the oxide surface into account, and we compare the analytical soultion of this model with the Poisson-Boltzmann and the Debye-Hückel model.**

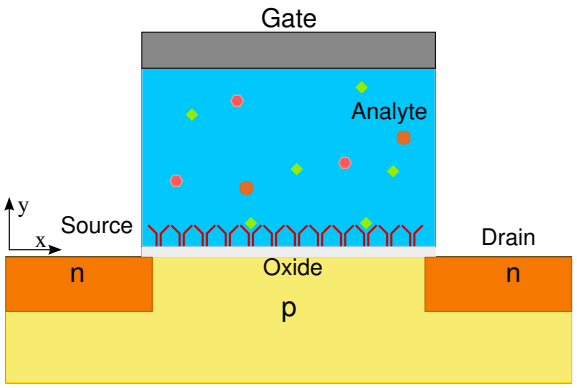

Fig. 1. Scheme of suspend gate field-effect transistor.

Introduction

The need for fast, cheap, reliable, and in-situ detection of DNA, antibody, protein and tumor markers, also known as "point of care" applications, requires new technological approaches. Today the detection of DNA needs several complex and time consuming steps, like amplification of the DNA by polymerase chain reaction (PCR) or reverse transcription (RT), followed by a procedure to add certain molecules which are able to fluroescent or radiate (called labeling), and at last an optical read out of the experimental data with a microarray reader [1], [2].

One promissing approach is to exchange the optical detection mechanism by an electrically working principle [3]–[9]. The field-effect based approach has several advantages over the optical method. The application of a field-effect transistor eases the integration of amplifying and analyzing circuits on the same chip, thus reducing the costs for the readout equipment. Additionally, the use of semiconductor process technology enables mass production and a corresponding huge decrease in price per device.

In this work the experimental data of a biosensor for detecting DNA are studied via three different models. The biosensor is a suspend gate field-effect transistor (SGFET). This device is a MOSFET with a raised gate and an empty space beneath it (see Fig. 1). Within this empty gap the gate-oxide layer is chemically modified with single stranded DNA which is able to hybridize with a complementary strand. Due to the intrinsic charge of the phosphate groups (minus one elementary charge per group) of the DNA large shifts in the transfer characteristics are induced. Thus label-free, time-resolved, and in situ detection of DNA is possible. Interestingly the commonly used Poisson-Boltzmann models are not able to reproduce the experimental data, while the Debye-Hückel model [10] works, although its validity in the used regime is questionable.

Finally we introduce an extended Poisson-Boltzmann formulation which takes the closest possible approach between ions into account. In an aqueous solution the salt ions are covered with water molecules. Due to the thereby increased effective ion radius there is a minimum distance between the ions and the oxide surface, called outer Helmholtz plane (OHP). Within this OHP there is no screening.

Experimental Data

In the work of Harnois [11] 60 oligo-deoxynucleotides (ODN), also known as single stranded DNA, were attached onto a glutaraldehyd coated nitride layer. Then one test run with mismatched ODNs and one test run with matching ODNs were carried out. The runs with the mismatching DNA show no relevant change in the output curves, while for the matching single stranded DNA a big shift in the threshold voltage becomes visible. The results show two interesting properties.

978-1-4244-3927-0/09/$25.00 ©2009 IEEE

Firstly, a threshold voltage shift of about $800\,\mathrm{mV}$ between the probe curve and the target transfer curve and, secondly, the probe transfer curve lies in the middle between target and reference. The average threshold voltage shift is in a range from several mV to $100\,\mathrm{mV}$ [12], depending on the buffer concentration, the $800\mathrm{mV}$ shift is quite big and the Poisson-Boltzmann regime shows a big shift between reference and probe/target ($\sim 100\,\mathrm{mV}$), but a much smaller shift between probe and target ($10 - 20\,\mathrm{mV}$) [2].

Simulation

First a Poisson-Boltzmann model was utilized which treats the buffer as continuous ion concentrations weighted with Boltzmann type terms ($e^{-\frac{qV}{k_B T}}$) (Fig. 3), combined with a space charge density that corresponds to 60 base pairs (probe) and 120 base pairs (target).

$$\begin{aligned}\epsilon_0 \nabla \cdot (\epsilon_{Ana} \nabla \psi(x,y)) &= -\sum_{\xi \in S} \xi\ q\ c_\xi^\infty\ e^{-\xi \frac{q}{k_B T}(\psi(x,y)-\psi_\mu)} \\ &\quad +\rho_{Space}(x,y) \qquad (1)\end{aligned}$$

k_B denotes Boltzmann's constant, T the temperature in Kelvin, and $\xi \in S$, where S contains the valences of the ions in the electrolyte. ϵ_0 describes the permittivity of vacuum, and q denotes the elementary charge. ψ_μ is the chemical potential. c_σ^∞ is the ion concentration in equilibrium, while $\epsilon_{Ana} \approx 80$ is the relative permittivity of water.

The second model also uses the Poisson-Boltzmann description but assumes a sheet charge density at the oxide-analyte interface (Fig. 4).

$$\begin{aligned}\epsilon_0 \nabla \cdot (\epsilon_{Ana} \nabla \psi(x,y)) &= -\sum_{\xi \in S} \sigma\ q\ c_\xi^\infty\ e^{-\xi \frac{q}{k_B T}(\psi(x,y)-\psi_\mu)} \\ &\quad +\sigma_{Sheet}(x)\,\delta(y - y_0) \qquad (2)\end{aligned}$$

The third model uses the Debye-Hückel formulation which can be derived by linearizing the Poisson-Boltzmann model (Fig. 5).

$$\begin{aligned}\epsilon_0 \nabla \cdot (\epsilon_{Ana} \nabla \psi(x,y)) &= \frac{2q^2}{k_B T}(\psi(x,y) - \psi_\mu) \sum_{\xi \in S} \xi^2 c_\xi^\infty \\ &\quad +\rho_{Sace}(x,y) \qquad (3)\end{aligned}$$

Discussion

Fig. 3, Fig. 4, and Fig. 5 show the transfer characteristics for the unprepared SGFET (reference), the prepared but unbound (probe), and when the DNA has bound to functionalized surface (target), respectively. For better comparison between experimental data and our simulation, the curves of the experiment are in discrete grey tones included. As can be seen for Fig. 3 and Fig. 4, even for the low salt concentration of $0.6\,\mathrm{mmol}$, the shift between the reference curve and the probe/target is bigger than between the probe and target curves. This behavior complies with the observations by [2] and is attributed to the nonlinear screening of the used models. Looking at Fig. 6 and Fig. 7 shows that doubling the charge at the interface does not lead to a doubled potential shift. Nevertheless there is a bigger shift for the sheet charge model due to the description of the DNA charge as sheet with infinite small height. Therefore less screening compared to the space charge model that distributes the same amount of charge over $20\,\mathrm{nm}$ takes place.

However, just by decreasing the salt concentration it is impossible to fit the experimental data. Nevertheless the Debye-Hückel model shows acceptable agreement with the experimental data for the same parameters as in the Poisson-Boltzmann description (Fig. 5). Here, doubling the amount of charge leads to twice the potential shift Fig. 8 because of the linear screening term in the model (3).

In order to understand why the Poisson-Boltzmann model fails and the Debye-Hückel model works, one hast to look for the validity constraints of the used models. For instance, assuming a volume of $10{\cdot}10{\cdot}20\,\mathrm{nm}^3$ for a single 60 bases DNA strand and one mmol sodium-chloride bulk concentration leads to an average concentration of about one sodium/chlorine atom within this given volume. So there will be no strong nonlinear screening in this regime. The Poisson-Boltzmann model treats the salt concentration as continuous quantity, so it is overestimating the screening and therefore is not valid for small salt concentrations.

The Debye-Hückel model can be derived by expanding the exponential terms into a Taylor series and neglecting all terms higher than second order [10]. According to the laws of series expansion $\frac{q\Psi}{k_\mathrm{B} T} \ll 1$ and thus the potential has to be small compared to the thermal energy. By treating the ions as infinite small point charges, the mean distance between the ions in the solution must be big and therefore the bulk salt concentration low. However, even though only one of the constraints is fullfilled, the Debye-Hückel model is able to fit the data.

Additionally we investigated a modified Poisson-Boltzmann model. This modified model takes the average closest possible approach of two ions within the liquid into account and is able to reproduce the Stern layer, where no screening takes place [2]. For better comparison to the other two models we study the one-dimensional analytical solutions for the Debye-Hückel, the Poisson-Boltzmann, and the extended Poisson-Boltzmann model.

Reformulating the Laplace term to

$$\frac{d\varphi^2}{dx^2} = -\frac{dE}{dx} = E \cdot \frac{dE}{d\varphi} \qquad (4)$$

and transforming the equations with

$$\varphi = \frac{q\psi}{k_\mathrm{B} T} \quad \text{and} \qquad (5)$$

$$\frac{1}{\lambda^2} = \frac{2qc_0}{k_\mathrm{B} T \epsilon_0 \epsilon_\mathrm{Ana}}\ , \qquad (6)$$

leads to the following differential equations:

$$E \cdot \frac{dE}{d\varphi} = \frac{1}{\lambda^2} \sinh(\varphi) \quad (7)$$

for the Poisson-Boltzmann model [13],

$$E \cdot \frac{dE}{d\varphi} = \frac{1}{\lambda^2} \varphi \ , \quad (8)$$

for the Debye-Hückel model.

Integrating these equations twice gives the following solutions:

$$\varphi(x) = 2 \ln \left(\frac{1 + e^{-x/\lambda} \tanh(\varphi_0/4)}{1 - e^{-x/\lambda} \tanh(\varphi_0/4)} \right) \quad (9)$$

$$E(x) = \frac{4}{\lambda} \frac{e^{-x/\lambda} \tanh(\varphi_0/4)}{1 + e^{-x/\lambda} \tanh(\varphi_0/4)} \ , \quad (10)$$

for the Poisson-Boltzmann model and

$$\varphi(x) = \varphi_0 \, e^{-x/\lambda} \quad (11)$$

$$E(x) = \varphi_0/\lambda \, e^{-x/\lambda} \quad (12)$$

for the Debye-Hückel model.

Our proposed extended Poisson-Boltzmann model is formulated as

$$E \cdot \frac{dE}{d\varphi} = \frac{2}{\lambda^2} \frac{(a - (a-1)\cosh(\varphi/2)) \sinh(\varphi/2)}{((1-a) + a\cosh(\varphi/2))^3} \quad (13)$$

or simplified,

$$E(\varphi) = \frac{2}{\lambda} \frac{\sinh(\varphi/2)}{1 - a + a\cosh(\varphi/2)}, \quad (14)$$

where a is the closest average distance between ions. For the limit $a \to 0$ the initial Poisson-Boltzmann formulation is obtained. Fig. 2 shows the behavior of the extended Poisson-Boltzmann model. Close to the surface the extended model shows no screening, also known as the Stern layer [14]. The stern layer arises from the salt ions which are covered in a shell of water molecules. This water shell causes a minimum distance to the oxide surface (OHP) and generates a region without screening. While when one gets outside the OHP strong nonlinear screening takes place (Gouy-Chapman diffusive layer). Fig. 2 confirms that for $\mathrm{a} = 0$ the potential of the Poisson-Boltzmann model is recovered. Increasing a leads to reduced screening and generates for $\mathrm{a} = 0.28$ a similar behavior like the Debye-Hückel model. For better comparability the calculations were carried out in dimensionles units and with the same surface charge.

Conclusion

Decreasing the salt concentration does not improve the result of the Poisson-Boltzmann model. The reason is that due to nonlinear screening doubling the charge density does not lead to twice the potential shift (shown in Fig. 6). The Debye-Hückel formulation produces the best fit. Two conditions for this model must be met [10]. Firstly, the salt concentration has to be low and, secondly, the potential in the exponential

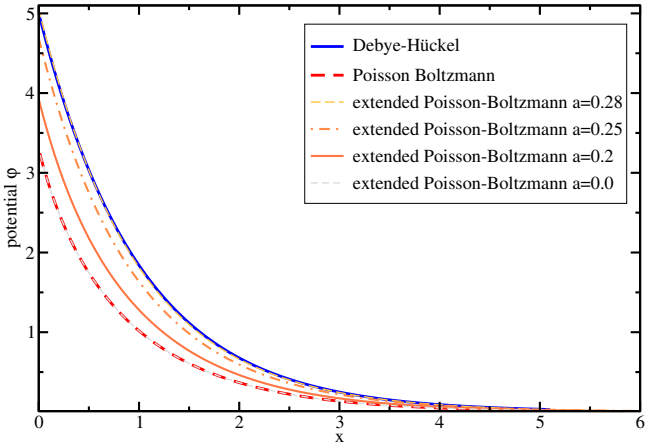

Fig. 2. Analytic solution of different models at same interface charge.

terms has to be small compared to $\mathrm{k_B T}$. Despite the fact that the potential is not small enough to satisfy the linear model, it is able to reproduce the experimental data. A possible reason is that the Poisson-Boltzmann model overestimates screening. Indeed, for small salt concentrations the Poisson-Boltzmann model breaks down at high potential values, when there are not enough ions to cause screening. Therefore, the physical behavior is far more complex and requires further investigation.

Acknowledgement

This work was supported by the Austrian Science Fund FWF, Project P19997-N14.

References

[1] M. C. Pirrung, "How to make a DNA chip," *Angew. Chem. Int. Ed.* **41**, 1276 (2002).

[2] M. W. Shinwari *et al.*, "Study of the electrolyte-insulator-semiconductor field-effect transistor (EISFET) with applications in biosensor design," *Microelectronics Reliability* **47**(12), 2025 (2007).

[3] K. Y. Park *et al.*, "Development of FET-type albumin sensor for diagnosing nephritis," *Biosensors and Bioelectronics* **23**, 1904 (2008).

[4] K. Park *et al.*, "BioFET sensor for detection of albumin in urine," *Electronic Letters* **44**(3) (2008).

[5] S. Gupta *et al.*, "Detection of clinical relevant levels of protein analyte under physiologic buffer using planar field effect transistors," *Biosensors and Bioelectronics* **24**, 505 (2008).

[6] Z. Gao *et al.*, "Silicon nanowire arrays for label-free detection of DNA," *Analytical Chemistry* **79**(9), 3291 (2007).

[7] H. Im *et al.*, "A dielectric-modulated field-effect transistor for biosensing," *Nature Nanotechnology* **2**(7), 430 (2007).

[8] E. Stern *et al.*, "Lable-free immunodetection with CMOS-compatible semiconducting nanowires," *Nature Letters* **445**(1), 519 (2007).

[9] A. Girard *et al.*, "Transferrin electronic detector for iron disease diagnostics," *IEEE Sensors* page 474 (2006).

[10] P. Debye and E. Hückel, "Zur Theorie der Elecrolyte: I. Gefrierpunktserniedrigung und verwandte Erscheinungen.," *Physikalische Zeitschrift* **24**(9), 185 (1923).

[11] M. Harnois *et al.*, "Low concentrated DNA detection by SGFET," in *Transducers & Eurosensors* (2007) 1983–1986.

[12] A. Poghossian *et al.*, "Possibilities and limitations of label-free detection of DNA hybridization with field-effect-based devices," *Sensors and Actuators, B: Chemical* **111-112**, 470 (2005).

[13] B. Derjaguin and L. Landau, "Theory of the stability of strongly charged lyophobic sols and the adhesion of strongly charged particles in solutions electrolytes.," *Russian Journal of Experimental and Theoretical Physics (ZhETF)* **11**(15), 663 (1945).

[14] O. Stern, "Zur Theorie der elektrolytischen Doppelschicht," *Zeitschrift für Elektrochemie und angewandte physikalische Chemie* **30**, 508 (1924).

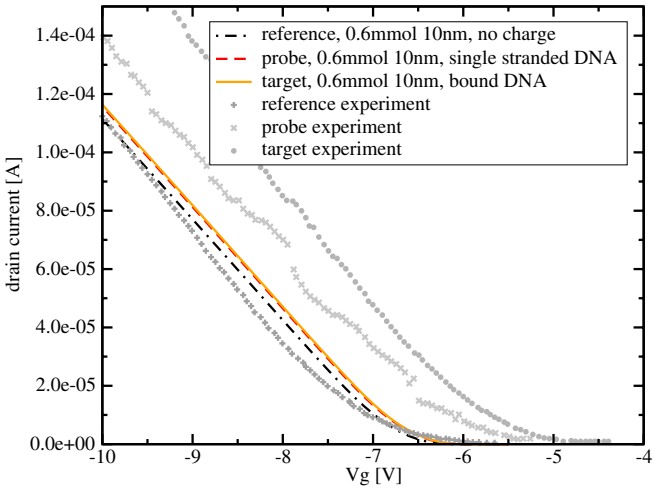

Fig. 3. Transfer characteristics of a SGFET for Poisson-Boltzmann model and DNA charge modeled via space charge density.

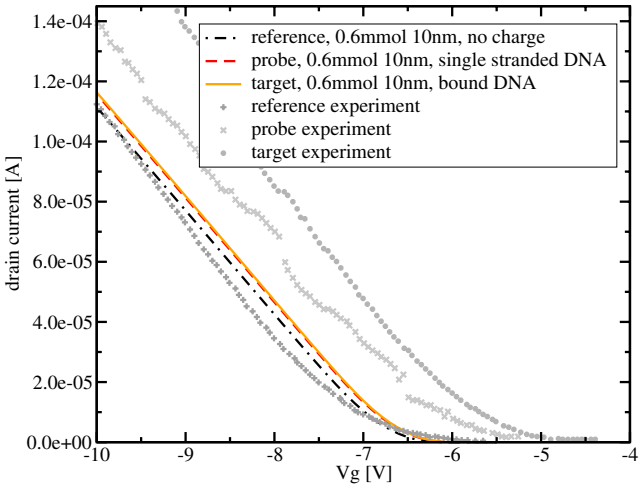

Fig. 4. Transfer characteristics of a SGFET for Poisson-Boltzmann model and DNA charge modeled via sheet charge density.

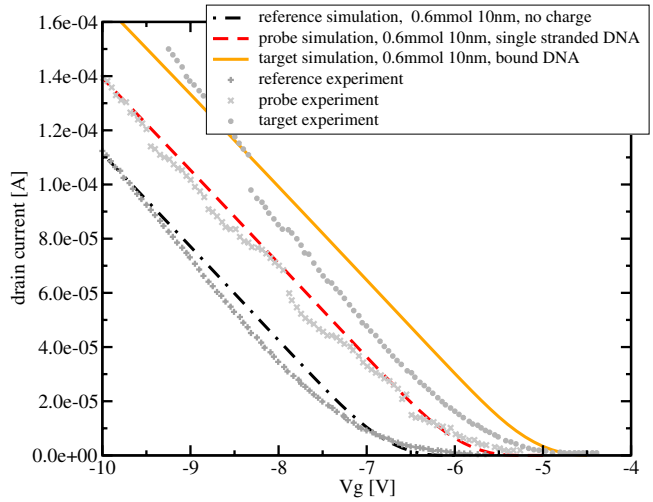

Fig. 5. Transfer characteristics of a SGFET for Debye-Hückel model and DNA charge modeled via space charge density.

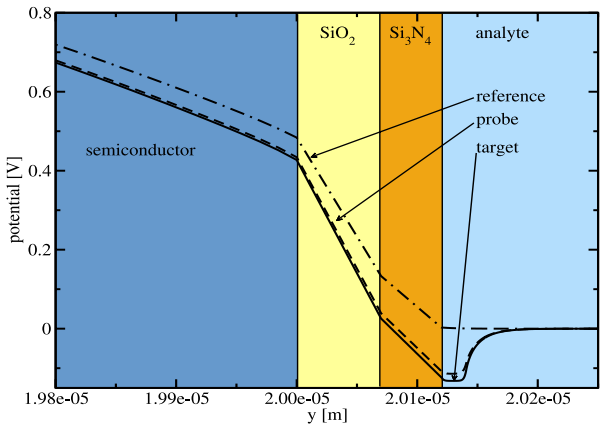

Fig. 6. Potential for the Poisson-Boltzmann model with space charge, starting from the semiconductor (left) and ending in the analyte (right). It can be seen that doubling the charge does not lead to twice the potential shift due to nonlinear screening.

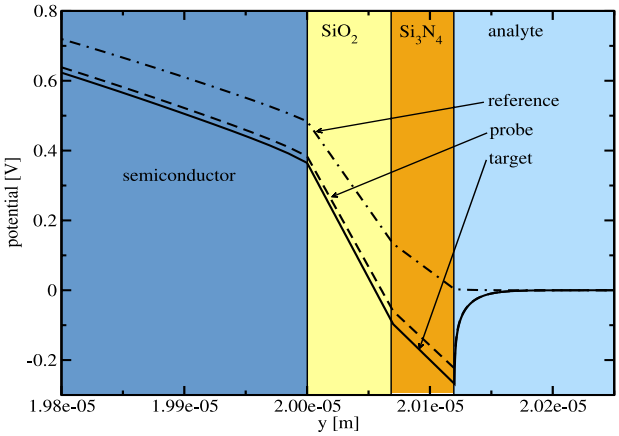

Fig. 7. Potential for the Poisson-Boltzmann model with sheet charge, starting from the semiconductor (left) and ending in the analyte (right). Here the shift is a bit increased but far away from the values from the measurement. However, also here doubling the charge does not lead to twice the potential shift due to nonlinear screening.

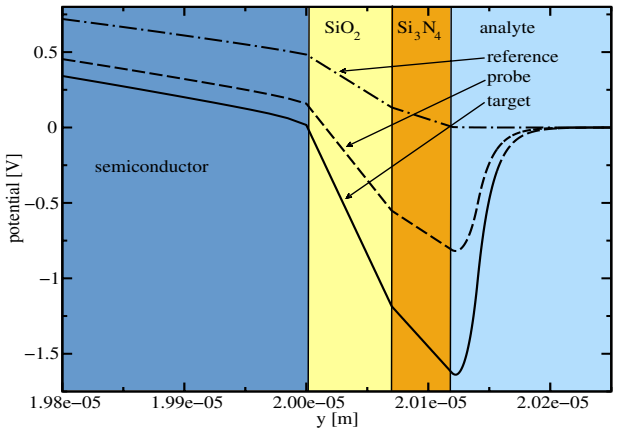

Fig. 8. Potential for the Debye-Hückel model with space charge, starting from the semiconductor (left) and ending in the analyte (right). It can be seen that doubling the charge leads to twice the potential shift due to the weaker linear screening.